Available online at www.sciencedirect.com
ScienceDirect
Dyes and Pigments 74 (2007) 512–518
DYES and PIGMENTS
www.elsevier.com/locate/dyepig

The removal of reactive dye printing compounds using nanofiltration

Irena Petrinić [a,*], Niels Peder Raj Andersen [b], Sonja Šostar-Turk [a], Alenka Majcen Le Marechal [a]

[a] University of Maribor, Faculty for Mechanical Engineering, Department of Textile Materials and Design, Smetanova ulica 17, SI-2000 Maribor, Slovenia
[b] Section of Chemistry, Aalborg University, Sohngaardsholmsvej 57, DK-9000 Aalborg, Denmark

Available online 9 January 2007

Abstract

A synthetically prepared reactive dye print wastewater, mimicking real wastewater obtained from a local textile mill, was treated by nanofiltration using an NFT-50 membrane in a plate and frame module configuration at different cross-flow velocities (0.4, 0.6 and 0.8 m/s) and pressures (2–15 bar). The nanofiltration membrane was evaluated for membrane fouling, permeate flux and its suitability for removing colour, conductivity, Na^+ ions and COD as a function of operating pressure and feed concentration. The permeate separation efficiency was monitored by measuring the removal efficiency of colour, conductivity, Na^+ ions and COD retention. The membrane achieved high dye retention for each of the four dyes (from 99.4 to 99.9%) and electrolytes used (63–73%). The retention of organic substances varied between 20 and 50%, depending on the pressure used; higher retentions were achieved at higher pressure and by using higher cross-flow velocities.

Keywords: Nanofiltration; Membrane; Wastewater after reactive printing; Reactive dye; Concentration polarization

1. Introduction

Textile printing is an important method for decorating textiles. Cellulosic fibres are the most commonly printed substrate and reactive dyes are, by far, the most commonly used colourants in textile printing [1]. At the end of printing, when the print is washed and rinsed to remove surplus colourant and auxiliaries, some 200 L of water per kg of textile is typically consumed. There is an obvious need to save water; water reuse is also possible as many washing and rinsing operations can employ water of lower quality than fresh water. This means that processed water (colourless or with very low coloured waste) can be reused in the rinsing process, as long as its contamination is lower than the resulting wastewater produced by the process itself [2,3]. However, most of the auxiliary components must be removed sufficiently to provide a wash water quality that is suitable for effective washing of the fabric [4].

While reused water has often been used in the rinsing and washing processes, focus has also been given to reusing the wastewater after dyeing [5]. Pilot plant trial processes have been investigated using reverse osmosis (RO), nanofiltration (NF) and ultrafiltration (UF) from continuous washing processes subsequent to reactive dyeing processes [6,7]. It was found [2] that UF could not completely decolourise wastewater as it did not remove low M_r dyes; a combination of RO and NF was required in order to secure decolourised and desalinated wastewater. RO membranes desalinate wastewater effectively (NaCl retention of 93%) and produce a colourless permeate and nanofiltration shows great potential for the direct reuse of such wastewaters. While water and (most of the) sodium chloride pass through a nanofiltration membrane, most divalent ions and dye molecules are rejected. It is well-known that after nanofiltration of simulated wastewater, 99% colour

* Corresponding author. Tel.: +386 2 220 7906; fax: +386 2 220 7990.
E-mail address: irena.petrinic@uni-mb.si (I. Petrinić).

0143-7208/$ - see front matter © 2006 Elsevier Ltd. All rights reserved.
doi:10.1016/j.dyepig.2006.11.003

removal and 84% electrolyte recovery were achieved; thus, the direct nanofiltration of dye bath wastewaters has been shown to be a realistic method for the treatment of such wastewater [8]. In addition to the separation obtained in nanofiltration, permeate flux through the membrane is an important parameter for the design of a filtration unit. This parameter is defined as the permeate flow through the membrane per unit surface area of the membrane. The presence of organic and inorganic solutes causes a lower permeate flux than that obtained for pure water. Two phenomena are important: the immediate decline in permeate flux when applying the solution to be filtered and the stability of the flux as a function of time [9].

In this work, cross-flow nanofiltration membrane filtration was used to treat a synthetically prepared wastewater that was similar to the textile effluent produced at the end of printing with reactive dyes. The effect of individual components was investigated with regard to the permeate flux. The extent of reactive dye and sodium ion retention, COD, and conductivity were determined in order to monitor the membrane's separation efficiency.

2. Materials and methods

Four different reactive dyes were used namely C.I. Reactive Red 24 (a commercially available product of CHT Bezema, Switzerland), C.I. Reactive Orange 12, C.I. Reactive Blue 19 and C.I. Reactive Black 5 (supplied by DyStar, Germany); the chemical structures of the dyes used are presented in Fig. 1. *CHT-Alginate MV* and *Rapidoprint XRN Pearls* were supplied by CHT R. Beitlich GMBH, Germany. *Rapidoprint XRN Pearls* is a weak oxidizing agent used in printing to offset the reactive dye's sensitivity to reduction during steaming. $NaHCO_3$, Na_2CO_3 and urea were provided by a local factory.

2.1. Composition of the synthetically prepared textile wastewater

The simulated wastewater studied was prepared according to the washing process performed after reactive printing on textiles. The substances removed whilst washing off the prints, which end up in the wastewater, are thickener, unfixed dye and auxiliaries applied to the material as part of the printing process. The concentration of these components in the wash water depends on the component's concentration in the printing paste formulation. The basic printing recipe (concentrations before application) is shown in Table 1.

Alginate thickener was used (viscosity level 7%) for 3preparing the printing pastes. Print pastes were prepared by stirring the thickening agent in softened water. After the alginate had been rising for approx. 2 h, the other components were then added by stirring into the alginate solution. The amount of reactive dye added to the print paste depended on the depth of shade and hue desired: 150 g/L, 100 g/L, 150 g/L and 100 g/L for C.I. Reactive Orange 12, C.I. Reactive Red 24, C.I. Reactive Blue 19, and C.I. Reactive Black 5, respectively.

Simulation of the printing process was done in the laboratory using direct printing. The size of the printing screen was 40 × 30 cm and the mass of the printing paste applied during printing was 50 g. The mass of the printed fabric was 18.6 g; after printing, the fabric was dried for 5 min at 60 °C, steamed at 102 °C for 8 min and then for 15 min at 90 °C. Using a fabric:water ratio of 1:15, the amount of water required to wash-off the unfixed thickeners and dye from the print was 745.2 g. Synthetic wastewaters were prepared at a ratio 1:15 of coloured printing paste to water. The amount of each component was recalculated on the basis of the original recipe, as given in Table 1. Table 2 presents the composition of the synthetically

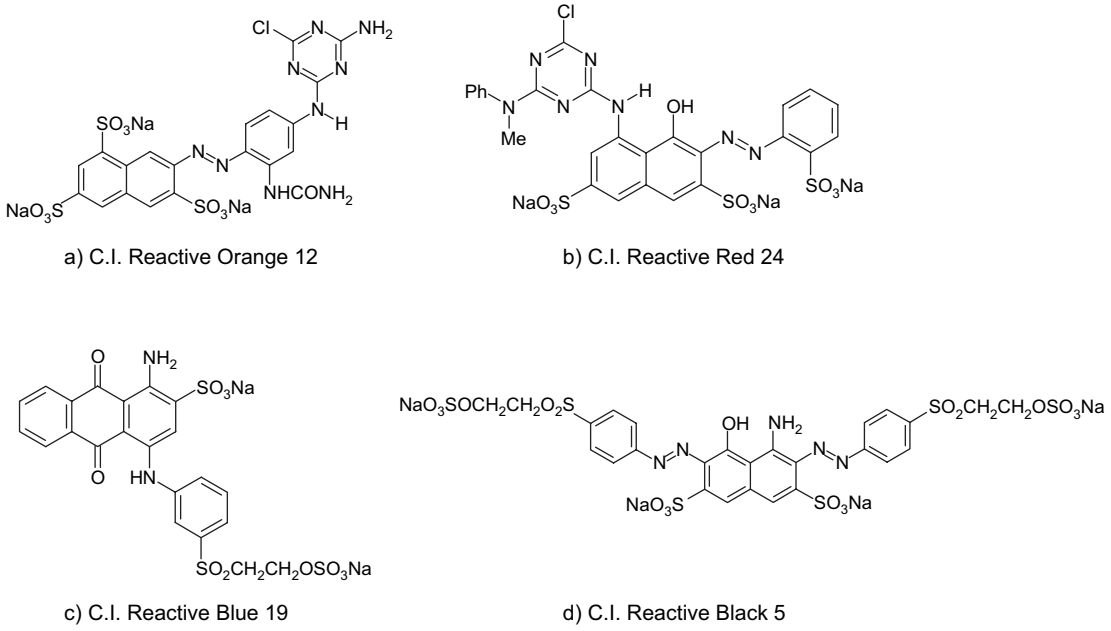

Fig. 1. Dye structures.

Table 1
Basic printing recipe

Print paste	Mass (g)
Urea	15
$NaHCO_3$	2
Na_2CO_3	1
Rapidoprint	1
Alginate 7%	39
Demin. water	42
	100
Coloured printing paste	
Printing paste	90
Reactive dye	*X*
Demin. water	*Y*
	100

prepared wastewater in which the concentrations of the auxiliaries were kept constant and only the dye (C.I. Reactive Orange 12, C.I. Reactive Red 24, C.I. Reactive Blue 19 and C.I. Reactive Black 5) concentration (1.2 g/L, 0.8 g/L, 1.2 g/L, and 0.8 g/L, respectively) was varied. The solution contained one of the reactive dyes in each experiment and the pH of the solutions was constant at 10.6. The model solutions used are titled: ww-C.I. Reactive Orange 12, ww-C.I. Reactive Red 24, ww-C.I. Reactive Blue 19 and ww-C.I. Reactive Black 5.

The removal efficiency of the membrane is generally expressed by rejection (R) defined by Eq. (1).

$$R = 100\left(1 - \frac{c_p}{c_b}\right) \quad (1)$$

where c_p is the concentration of the permeate and c_b the bulk concentration.

2.2. Filtration unit

The experiments were carried out in a modified DDS Lab 20 unit (Fig. 2) in which membranes were installed in series; the system was operated in a batch mode. For performance evaluation, experiments were carried out in total recycle mode of filtration (TRMF) in which both the retenate

Table 2
Synthetic wastewater (model solution)

No.	Component	M (g mol^{-1})	γ (g L^{-1})
1	Urea	60	8.4
2	$NaHCO_3$	84	1.1
3	Na_2CO_3	106	0.56
4	Rapidoprint (nitrobenzenesulphonate)	202	0.56
5	Sodium alginate (7% solution)	100–500 kDa	22
6	C.I. Reactive Orange 12	739	1.2
7	C.I. Reactive Red 24	788	0.8
8	C.I. Reactive Blue 19	626	1.2
9	C.I. Reactive Black 5	991	0.8

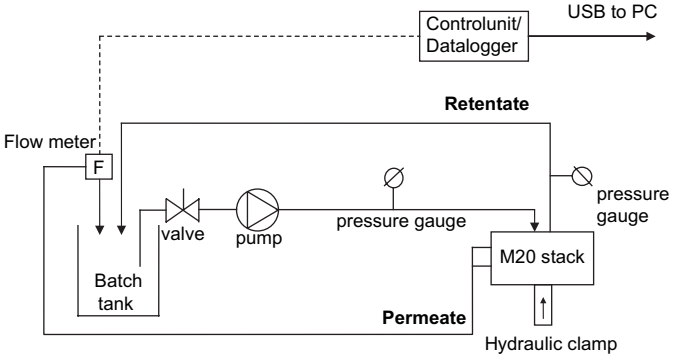

Fig. 2. Schematic flow diagram of the membrane filtration system.

(representing that portion of the feed solution that is retained on the high-pressure side of the membrane) and the permeate (representing that portion of the feed solution passing through the membrane) are recycled into the feed tank. Thus, the feed quality is assumed to be constant since the feed volume is kept constant throughout the experiment. The TRMF tests were conducted using 4–6 L of feed wastewater. The filtration duration ranged from 1 to 3 h, until a steady state permeate flux was obtained. The variations of permeate flux with step increment of transmembrane pressure (TMP) were studied at a cross-flow velocities of 0.4, 0.6 and 0.8 m/s. The TMP was set to 2 bar and stabilized flux was obtained after 10 min. The pressure was then raised to 4, 7, 10, 12 and 15 bar every 10 min to permit flux stabilization, until the flux became pressure independent. Before ending the tests, the permeates were sampled for further analysis, after the steady state was reached. A single pump was employed to provide both cross-flow flush and operational pressure for permeate production.

Nanofiltration was performed using the thin film membrane, NFT-50, supplied by Alfa Laval, Sweden, as a flat sheet with an area of 0.011067 m^2. The membrane has a sulfonated polyamide skin layer on top of a polyether support. The M_w cut-off (MCWO – M_wt of the uncharged solutes showing 90% rejection) was determined to be 159 Da. The detailed procedure has been reported previously [10]. The hydraulic permeability, L_p, was determined by measuring the permeate flux as a function of applied transmembrane pressure; the slope of the obtained straight line gives the water permeability value for the membrane and determines how fast the component is transported through the membrane. This was found to be 8.5 L m^{-2} h^{-1} (LMH). The permeability values are within the range normally obtained with NF membranes available in the market (1–50 L m^{-2} h^{-1}/bar) [11]. Streaming potential measurements have shown the membranes to be negatively charged within the pH range studied [10].

2.3. Methods

The effect of the components in the model solution on the colour, conductivity, Na^+ ion concentration and COD

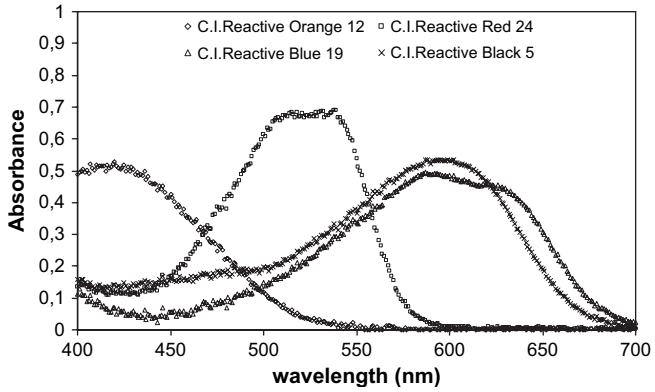

Fig. 3. λ_{max} of each reactive dye used.

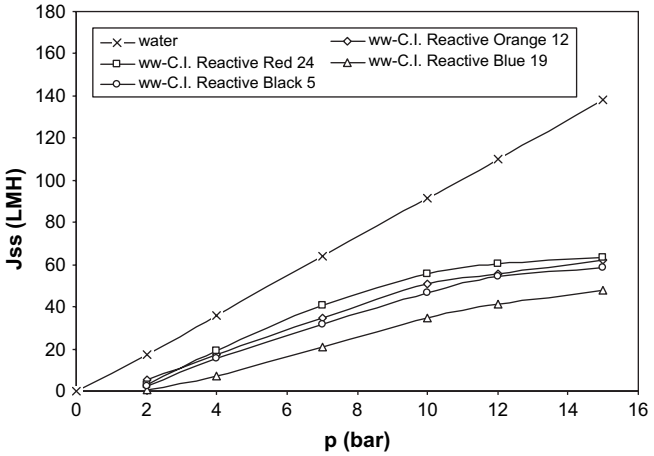

Fig. 4. Permeate flux of ww-C.I. Reactive Orange 12, ww-C.I. Reactive Red 24, ww-C.I. Reactive Blue 19 and ww-C.I. Reactive Black 5 using NFT-50 membrane, cross-flow 0.4 m/s.

separation efficiency during filtration was investigated. Spectroscopic analysis of the prepared effluents was carried out using a Varian Cary 50. The wavelength of maximum absorption (λ_{max}) of each reactive dye was determined (Fig. 3), and a calibration plot of absorbance versus dye concentration at the appropriate λ_{max} for each reactive dye was determined. The equation of the line for each calibration plot, $y = ax + b$ (y = absorbance, a gradient, x = concentration) was then used to calculate the concentration of residual solution from the absorbance determination (Table 3).

COD was measured according to the Standard method [12]. The Na^+ ion concentration was determined by atomic absorption spectrometry (Perkin Elmer 1100B) using acetylene as fuel gas at a flow rate of 2.5 L/min and compressed air at a flow rate of 8.0 L/min as oxidant. The hollow cathode lamp's current was 10 mA and absorption was measured at 589.0 nm (slit 0.2 nm). The samples were diluted in 100 mL flasks and cesium chloride solution was added as ionization suppressant.

3. Results

3.1. Membrane permeate flux

The variation of the permeate flux with TMP membrane and all four model solutions is presented in Fig. 4. It is evident that membrane fluxes were lower than for the corresponding pure water flux (measured with distilled water as feed); this is a phenomenon that can be related to the presence of organic and inorganic solutes [9]. The flux reduction can be divided into two separate parts. Firstly, fluxes are reduced due to the effect of concentration polarization in which, retained solutes at the membrane surface result in an accumulation of particles in a mass transfer boundary layer adjacent to the membrane surface, which affects the flux. Concentration polarization can be minimized by using a turbulent flow regime (using turbulence promotors or relatively high cross-flow velocities). Secondly, solutes accumulating at the surface reduce solvent activity which, in turn, reduces the solvent flow through the membrane. This can be represented as a reduction in the effective transmembrane pressure driving force, due to an osmotic pressure difference between the filtrate and the feed solution adjacent to the membrane surface. This phenomenon is inevitable, but is reversible by a reduction in TMP, and hence fluxes.

Table 3
The equations of the dyes standard curves

Dyes	Equation
C.I. Reactive Orange 12	$y = 21.11x - 0.017$
C.I. Reactive Red 24	$y = 25.15x - 0.01$
C.I. Reactive Blue 19	$y = 8.21x - 0.003$
C.I. Reactive Black 5	$y = 33.9x - 0.089$

Both concentration polarization and osmotic pressure are reversible but might lead to membrane fouling. Above a certain TMP, fouling increases causing the flux to level off and to become pressure independent. The challenge for applying nanofiltration in such a demanding application as this is to find the particular conditions under which membrane fouling is minimized or avoided. Therefore, further experiments were carried out at variable cross-flow velocities.

Reduction of *concentration polarization* can occur by using optimized operating conditions. The operating conditions which influence productivity and rejection are transmembrane pressure, solute concentration and recirculation flow rate (cross-flow velocity) [13]. The cross-flow which limits the build-up of a solute is a crucial operational characteristic. The thickness of the layer adjacent to the membrane surface is primarily controlled by the cross-flow velocity. Increasing velocity generally increases the flux by increasing the rate at which the filter cake is swept away and cake resistance reduced. At higher flow velocities, higher pressures could be achieved with decreased amounts of fouling. Experiments using higher cross-flow velocities (0.6 and 0.8 m/s) were conducted for each model solution. Once again, stationary values of the flux were obtained within 30 min. The results of all other model solutions are tabulated in Table 4.

Steady state permeate flux as a function of cross-flow velocity from 0.4 to 0.8 m/s was observed at 10 bar and is shown in Fig. 5 for each membrane used. The observed increased flux

Table 4
Flux values (LMH) at different cross-flow velocities for ww-Orange, ww-Red, ww-Blue and ww-Black for NFT-50 membrane

p (bar)	ww-Orange			ww-Red			ww-Blue			ww-Black		
	0.4 m/s	0.6 m/s	0.8 m/s	0.4 m/s	0.6 m/s	0.8 m/s	0.4 m/s	0.6 m/s	0.8 m/s	0.4 m/s	0.6 m/s	0.8 m/s
2	5.4	6.9	10.7	3.1	7.1	11.5	0.4	2.2	2.3	2.3	3.6	8.4
4	17.2	27.3	28.6	19.3	22.0	30.4	7.2	14.5	19.5	15.3	17.8	24.9
7	34.6	53.6	57.1	40.8	44.8	59.3	20.7	35.2	38.1	31.8	37.9	49.7
10	50.8	73.3	78.8	55.8	63.9	76.6	34.5	51.3	56.5	46.8	54.9	69.7
12	55.9	77.3	87.2	60.5	72.5	86.4	41.1	60.7	67.5	54.2	64.5	84.6
15	62.2	84.0	93.4	63.3	77.7	92.9	48.1	68.6	79.2	58.3	73.7	100.8

at higher cross-flow velocities shows that the shear rate was sufficiently high to keep the concentration polarization layer small enough so that it does not restrict the permeate flux.

In nanofiltration, the retention of the ionic species results in an *osmotic pressure* build-up across the membrane. The osmotic pressure causes flux to decline, but this is due to reduced driving force rather than an increase in the resistance to mass transport. This can be expressed by the phenomenological equation for the water flux, originally introduced by Spiegler and Kedem [14], Eq. (2):

$$J_{SS} = L_p(\Delta P - \sigma \Delta \pi_{mem}) \tag{2}$$

where L_p is the water permeability, ΔP is the transmembrane pressure, σ is the reflection coefficient defined as $\sigma = 1 - c_p/c_m$ and $\Delta\pi_{mem}$ is the osmotic back-pressure due to the concentration differences across the membrane. The reflection coefficient represents the intrinsic salt rejection by the membrane. For the RO separations, σ was >0.98 and may be assumed equal to unity [15]. When intrinsic electrolyte rejection was significantly less than 0.98 (i.e. nanofiltration), the reflection coefficient should be used to more accurately predict the resultant transmembrane osmotic pressure [16]. The combined product of $\sigma\Delta\pi$ may be thought of as the 'effective trans-membrane' osmotic pressure drop, $\Delta\pi_m$.

Eq. (2) can be rearranged as Eq. (3)

$$\Delta\pi_m = \Delta P - \frac{J_{ss}}{L_p} \tag{3}$$

Osmotic pressure can be calculated by using the measured J_{SS} and Eq. (3). The influence of osmotic pressure for urea, *Rapidoprint* and dye/water solutions was minor. For example, at 10 bar, the concentration in the wastewater would result osmotic pressures of 0.12, 0.5 and 0.4 bar for urea, *Rapidoprint* and dye/water solutions, respectively. The extent to which osmotic pressure plays a role in electrolyte and alginate/water solution is much higher, resulting in 14 and 21.9% decline, respectively.

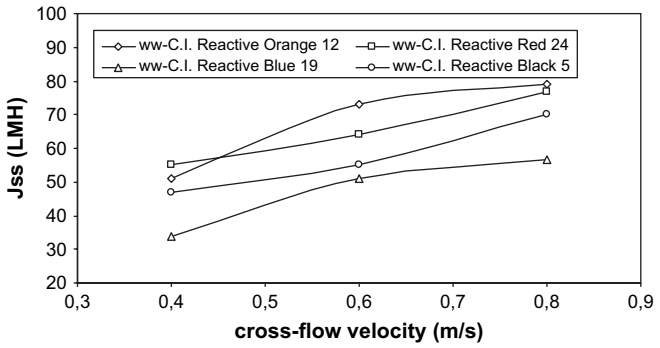

Fig. 5. Steady state permeate flux versus cross-flow velocity for cross-flow filtration from 0.4 to 0.8 m/s was observed at 10 bar for NFT-50.

From Fig. 4, it can be seen that at the start of filtration (2 bar) an immediate deviation of the permeate flux was observed from the pure water flux, for all model solutions. This could be due to particle–pore interactions causing an initial fouling of the membrane by pore narrowing, constrictions or plugging. These forms of fouling exist for solutions containing solutes that are relatively small compared to the mean pore size of the membrane, and where there is an electrostatic interaction. The model solutions used consist of high amounts of alginate, electrolyte ($NaHCO_3$ and Na_2CO_3), oxidants (nitrobenzene sulphate), urea and different types of reactive dyes. As expected at high pH values, the solution contains substantial concentration of the bivalent CO_3^{2-} ions and below pH 12.6 bicarbonate (HCO_3^-) ions are increasingly formed. Therefore, there will be strong repulsion between the membrane and the solution. The Na^+ ions have the capability of traveling to the membrane/water interface and effectively negating the zeta potential, thus destroying the barrier to the initial electro-kinetic potential. Sodium alginate is a linear polymer based on two monomeric units that dissociates in solution forming highly charged macromolecules or aggregates. Sodium alginate contains hydroxyl groups and in aqueous solution, will be negatively charged. Large single ions act as hydrophobic molecules, binding to a surface not only due to their charge, but also via Van der Waals forces. As aggregates of the polymer are unable to pass through the pores of the membrane, they will stay at the surface. There is also a tendency for dye molecule adsorption to occur at the membrane surface with increasing pH, possibly due to the aggregation and the formation of a strong and stable dye–electrolyte complex [17].

In order to identify the highest flux-reducing component in the model solution, the filtration of each compound was performed individually (*Rapidoprint*/water, urea/water, electrolyte/water, alginate/water and C.I. Reactive Red 24 and C.I. Reactive Blue 19/water) at the concentrations given in Table 2 (Fig. 6).

Urea/water solution had very little effect on flux, followed by the electrolytes and alginate/water solutions. The effect of the electrolyte/water solution can be attributed to concentration

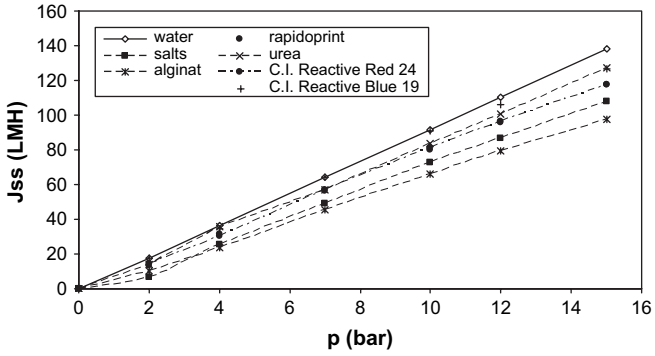

Fig. 6. Filtration by components, cross-flow 0.4 m/s.

polarization, while alginate/water can be considered to have created a thin gel layer on the surface and, therefore, imparted greatest reduction in flux. The reactive dyes had little effect on flux decline, due to their negative charge causing electrostatic repulsion.

3.2. Permeate quality

In Table 5 the results of bulk model solutions are presented in terms of conductivity, dye concentration, Na^+ concentration and COD.

Fig. 7 shows the retention values for colour, conductivity, sodium ion and COD at a cross-flow velocity of 0.4 m/s, pH = 10.6. High dye retention was obtained for all four dyes (from 99.4 to 99.9%) and both electrolytes (from 63 to 73%). Although dye retention did not change with pressure, electrolyte and sodium retention did. A high diffusive transport rate of ions through the membrane, compared to convective transport, is the reason that lower retention was found at low flux (lower pressure). With increasing flux, the contribution of convective transport becomes more important and rejection increases [18,19]. However, at high pressure the concentration polarization will also increase with increasing flux, resulting in a decrease in rejection. The counteracting contributions of increased convective transport and increased concentration polarization results in a constant rejection of the measured fluxes. Jiraratananon et al. [20] claimed that due to the superimposition effects of transmembrane osmotic pressure, a boundary layer was formed near the membrane surface which served as a resistance to electrolyte permeation. Negatively charged membranes may suffer large variations

Table 5
Characterisation of the model solutions

	pH	μ (mS cm^{-1})	c_{dyes} (mg L^{-1})	c^+_{Na} (mg L^{-1})	COD (mg mg L^{-1} O_2)
ww-C.I. Reactive Orange 12	9.4	3.39	0.98	1.46	9800
ww-C.I. Reactive Red 24	9.4	2.98	0.53	1.41	9500
ww-C.I. Reactive Blue 19	9.8	3.77	0.95	1.42	9600
ww-C.I. Reactive Black 5	9.5	2.74	0.58	0.92	8800

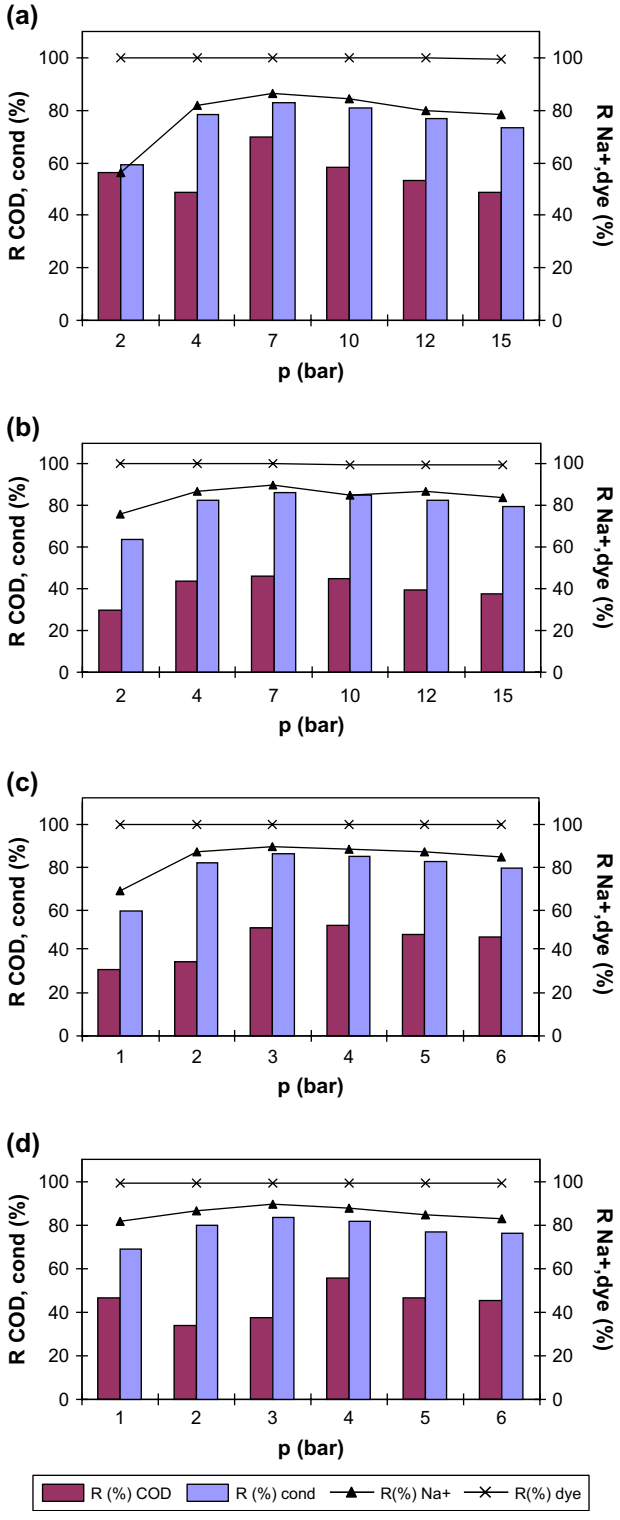

Fig. 7. Retention values, COD, conductivity, Na^+ concentration and dye, cross-flow 0.4 m/s, pH = 10.6. (a) ww-C.I. Reactive Orange 12; (b) ww-C.I. Reactive Red 24; (c) ww-C.I. Reactive Blue 19; (d) ww-C.I. Reactive Black 5.

in electrolyte rejection with increasing ionic strength, indicating that concentration polarization played an important role in damping out electrostatic repulsion. The neutral membranes used by Jiraratananon et al. [20] displayed low electrolyte

rejection since they had no surface charge and, as such, rejection depended mainly on the size of the solute and the morphology of the membrane.

The retention of organic substances and total carbon varied between 20 and 50%, depending on the pressure used; higher retention was achieved at higher pressure and by using higher cross-flow velocities. However, for ww-C.I. Reactive Orange 12 and ww-C.I. Reactive Black 5, highest retentions were achieved at a cross-flow of 0.6 m/s.

4. Conclusions

A decrease in permeate flow of around 50% originated from concentration polarization and dye adsorption. Flux decline can be minimized by a change in operational conditions. Cross-flow velocities indicated a significant effect on flux values, which increased with increasing cross-flow velocities. It can be concluded that the membrane achieved high dye retention (from 99.9 to 99.4%) for each of the four dyes and both electrolytes (63–73%) used. Dye retention was unaffected by pressure, but electrolyte and Na^+ retention was affected by pressure. The retention of organic substances varied between 20 and 50%, depending on pressure; higher retentions were achieved at higher pressure and by using higher cross-flow velocities. However, for ww-C.I. Reactive Orange 12 and ww-C.I. Reactive Black 5, the highest retentions were achieved at a cross-flow of 0.6 m/s. Thus, using an NFT-50 membrane, high retention of dye and electrolyte could be obtained at a pressure of 10 bar, where the permeate flux decline was between 30 and 55% of the water flux.

References

[1] Kumbasar EPA, Bide M. Reactive dye printing with mixed thickeners on viscose. Dyes and Pigments 2000;47(1–2):189–99.
[2] Schneider R. Minimization of water consumption in European textile dyeing and printing industry using innovative washing and recycling technologies. Innowash – confidential progress reports of EU project EKV1-CT2000-00049; 2004.
[3] De Vreese I, Van der Bruggen B. Cotton and polyester dyeing using nanofiltered wastewater. Dyes and Pigments [available online 2006].
[4] Brandon CA, Jernigan DA, Gaddis JL, et al. Closed cycle textile dyeing – full scale renovation of hot wash water by hyper-filtration. Desalination 1981;39(1–3):301–10.
[5] De Florio L, Giordano A, Mattioli D. Nanofiltration of low-contaminated textile rinsing effluents for on-site treatment and reuse. Desalination 2005;181:283–92.
[6] Bottger D, Klawuhn. Einsatz der membranetechnik zur Abwasserreinigung in der Textilveredlung mit Wasserkreislaufschliessung. In: Proceeding Bremer Kolloquium Produktionsintegrierter Umweltschutz; 2001. p. C37–9.
[7] Dvarionienė1 J, Stasiškienė Ž, Knudsen HH. Pilot scale membrane filtration study on water reuse of rinsing water after reactive cotton dyeing. Environmental Research, Engineering and Management 2003;3(25):3–11.
[8] Koyuncu I, Topacik D, Yuksel E. Comparative evaluation of the results for the synthetic and actual reactive dye bath effluent treatment by nanofiltration membranes. Journal of Environmental Science and Health, Part A – Toxic/Hazardous Substances and Environmental Engineering 2003;38(10):2209–18.
[9] Van der Bruggen B, Vandecasteele C. Flux decline during nanofiltration of organic components in aqueous solution. Environmental Science and Technology 2001;35:3535–40.
[10] Petrinic I, Pusic T, Mijatovic I, Sostar-Turk S. The characterisation of polymeric nanofiltration membranes. In: Third international textile, clothing and design conference, October 8th to 11th, 2006, Dubrovnik; 2006. p. 693–8.
[11] Bowen WR, Mohammad AW. A theoretical basis for specifying nanofiltration membranes – dye/salt/water streams. Desalination 1998;117:257–64.
[12] International standard. Determination of the chemical oxygen demand, reference number ISO 6060. Geneva, Switzerland: International Organization for Standardization; 1989.
[13] Mulder M. Basic principles of membrane technology. Dordrecht, The Netherlands: Kluwer Academic; 1991.
[14] Spiegler KS, Kedem O. Thermodynamics of hyperfiltration (reverse osmosis): Criteria for efficient membranes. Desalination 1996;1:311–26.
[15] Bhattacharjee S, Chen JC, Elimelech M. Coupled model of concentration polarization and pore transport in crossflow nanofiltration. AIChE Journal 2001;47:2733–45.
[16] Murthy ZVP, Gupta SK. Estimation of mass transfer coefficient using a combined nonlinear membrane transport and film theory model. Desalination 1997;109:39–49.
[17] Koyuncu I, Topacik D. Effect of cross flow velocity, feed concentration, and pressure on the salt rejection of nanofiltration membranes in reactive dye having two sodium salts and NaCl mixtures: model application. Journal of Environmental Science and Health, Part A – Toxic/Hazardous Substances and Environmental Engineering 2004;39(4):1055–68.
[18] Van der Bruggen B, De Vreese I, Vandecasteele C. Water reclamation in the textile industry: nanofiltration of dye baths for wool dyeing. Industrial and Engineering Chemistry Research 2001;40(18):3973–8.
[19] Shu L, Waite TD, Bliss PJ, Fane A, Jegatheesan V. Nanofiltration for the possible reuse of water and recovery of sodium chloride salt from textile effluent. Desalination 2005;172(3):235–43.
[20] Jiraratananon R, Sungpet A, Luangsowan P. Performance evaluation of nanofiltration membranes for treatment of effluents containing reactive dye and salt. Desalination 2000;130(2):177–83.